# Isonitriles as Alkyl Radical Precursors in Visible-Light Mediated Hydro– and Deuterodeamination Reactions

Irene Quirós,[†][a] María Martín,[†][a] Miguel Gomez-Mendoza,[†][e] María Jesús Cabrera-Afonso,[a] Marta Liras,[e] Israel Fernández,[c],[d] Luis Nóvoa,[a] Mariola Tortosa,*[a],[b],[d]

[a]   Organic Chemistry Department, Universidad Autónoma de Madrid (UAM), Avda. Francisco Tomás y Valiente 7, Cantoblanco 28049, Madrid (Spain).

[b]   Institute for Advanced Research in Chemical Sciences (IAdChem), Universidad Autónoma de Madrid (UAM), Avda. Francisco Tomás y Valiente 7, Cantoblanco 28049, Madrid (Spain).

[c]   Department of Organic Chemistry, Faculty of Chemistry, Complutense University of Madrid, 28040 Madrid (Spain).

[d]   Center of Innovation in Advanced Chemistry (ORFEO-CINQA).

[e]   Photoactivated Processes Unit, IMDEA Energy, Av. Ramón de la Sagra, 3 28935, Móstoles, Madrid (Spain)

†These authors contributed equally to this work

E-mail: mariola.tortosa@uam.es

**Abstract:** Herein, we report the use of isonitriles as alkyl radical precursors in light-mediated hydro- and deuterodeamination reactions. The reaction is scalable, shows broad functional group compatibility and potential to be used in late-stage functionalization. Importantly, the method is general for $C_\alpha$-1°, $C_\alpha$-2° and $C_\alpha$-3° alkyl isonitriles. For most examples, high yields were obtained through direct visible-light irradiation of the isonitrile in the presence of a silyl radical precursor. Interestingly, in the presence of an organic photocatalyst (4CzIPN) a dramatic acceleration was observed. In depth mechanistic studies using UV-vis absorption, steady-state and time-resolved photoluminescence, and transient absorption spectroscopy suggest that the excited state of 4CzIPN is able to sensitize the isonitrile through a single electron transfer.

## Introduction

In the last decade, the rapid expansion of visible-light photoredox catalysis has provided a new toolbox to form C-C and C-X bonds that were challenging or impossible using two electron processes. One of the attractive features of photoredox catalysis is its ability to successfully use ubiquitous yet traditionally inert functional groups as coupling partners in a variety of transformations.[1] Amines are abundant across natural products, pharmaceuticals, polymers and biomolecules. The number of commercially available primary amines, from simple to complex, makes them one of the most accessible native functional groups.[2] Although they represent an attractive feedstock for the preparation of functionalized molecules through C-N bond activation, their synthetic potential is not fully exploited and alternative ways are required to promote C-N bond cleavage.[3] The two most used approaches to promote visible-light mediated deaminations involve the use of pyridinium salts and electron rich imines. Pyridinium salts can undergo a single-electron reduction to form a carbon centered radical that has been engaged in a myriad of metal-catalyzed[4,5] and photoredox catalyzed functionalizations.[6,7] The pyridinium salts are formed in one step through condensation of primary amines with pyrilium salts. Consequently, only $C_\alpha$-1° and $C_\alpha$-2° amines can be used. Tetraalkyl ammonium salts can also undergo light-mediated single electron reductions but their use is limited to a few transformations using benzylic derivatives.[8] On the other hand, electron-rich imines are capable of undergoing single electron oxidation in the presence of a photoredox catalyst, under visible-light irradiation. This allows for the generation of a carbon centered radical through β-scission of an imidoyl radical intermediate and is limited to the use of $C_\alpha$-3°

amines.[9,10] Very recently, visible-light photocatalysis has also been used to trigger the dinitrogenation of 1,2-dialkyldiazenes through an energy transfer process.[11] Although impressive progress has been made, there is still a lack of deamination protocols that are general for $C_\alpha$-1°, $C_\alpha$-2° and $C_\alpha$-3° alkyl amine derivatives.

■ Light-mediated C-N cleavage from alkyl amine derivatives
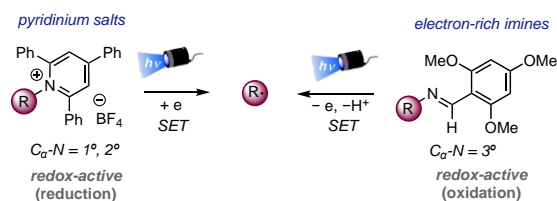


■ Isonitriles as alkyl radical precursors in light-mediated C-N cleavage (*this work*)
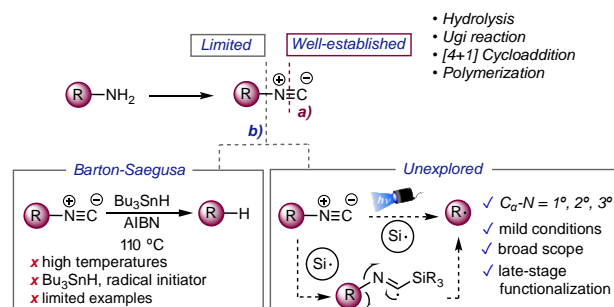


**Scheme 1.** Light-mediated C-N cleavage from alkyl amine derivatives and Barton-Saegusa hydrodeamination.

Searching for more general methods to promote C-N cleavage, we turned our attention to isonitriles. These chameleonic compounds are present in hundreds of secondary metabolites isolated from bacteria, fungi and marine sponges,[12] and are easily prepared from primary alkyl amines.[13] The functionalization of the N≡C multiple bond has been extensively exploited through Ugi multicomponent reactions, hydrolysis, [4+1] cycloadditions and polymerizations (disconnection **a**, Scheme 1).[14] However, the selective cleavage and functionalization of the C-N single bond is limited to the classical Barton-Saegusa reductive deamination (disconnection **b**, Scheme 1).[15] This reaction requires heating the isonitrile in refluxing benzene or xylene, in the presence of an excess of $^{n}Bu_3SnH$ and a radical initiator.[16] Inspired by this transformation, we wondered if isonitriles could be used as alkyl radical precursors in light-mediated transformations. Although isonitriles have recently shown visible-light photocatalytic activity,[17] their use as alkyl radical precursors through C-N bond cleavage under visible-light irradiation has not been studied to date. As a proof of concept to test this hypothesis we chose the hydrodeamination reaction. We anticipated that a silyl radical generated under visible light irradiation[18] could add to the isonitrile triggering the formation of an alkyl radical after β-fragmentation.[19] In this research article, we describe a general light-mediated hydrodeamination and deuterodeamination protocol that is operationally simple, requires mild conditions and shows broad functional group compatibility. Our method is general for $C_\alpha$-1º, $C_\alpha$-2º and $C_\alpha$-3º alkyl isonitriles and complements recently published hydrodeamination protocols.[20] Interestingly, in the presence of an organic photocatalyst we observed a dramatic acceleration of the reaction which opened the door to explore a different mechanistic scenario. Moreover, we believe that our findings will provide a platform to design further deamination reactions that could involve not only C-H bond formation but also C-C bond formation.

## Results and Discussion

To evaluate our hypothesis isonitrile **1a** was used as model substrate. We were pleased to find that just irradiating with a blue LED ($\lambda_{max}$ = 455 nm) a mixture of isonitrile **1a** and supersilane **2a** in MeCN, deaminated product **3a** was obtained in 77% yield (Table 1, entry 1).[21] An initial silane screening showed that tris(trimethylsilyl)silane **2a** afforded the best result, while other common silane sources such as tris(trimethylsilyl)silanol **2b**, triethylsilane **2c** or triphenylsilane **2d** did not afford the desired product (Table 1, entries 2-4). An increase in the concentration (0.2 M) had a beneficial effect on the yield of **3a** (entry 5). Additionally, the yield was almost quantitative using a commercially available blue 440 nm Kessil PR160L LED lamp (entry 6). Control experiments with no silane and no light (entries 7-8) confirm the necessity of these components to enable the hydrodeamination reaction.[22]

With suitable conditions in hand, we examined the scope and functional group tolerance of the light-mediated hydrodeamination (Scheme 2). We were pleased to find that the optimized conditions worked efficiently for $C_\alpha$-1º (**3h-i** and **3o-p**), $C_\alpha$-2º (**3b-g**) and $C_\alpha$-3º (**3j-n**) isonitriles. A wide variety of amino acids were also suitable substrates for the hydrodeamination through isonitrile activation (**3q-x**), including unprotected tyrosine (**3w**) and tryptophan (**3x**) derivatives, and

**Table 1.** Optimization of Reaction Conditions[a]



| (TMS)₃Si—H | (TMS)₃Si—OH | Et₃Si—H | Ph₃Si—H |
|---|---|---|---|
| **2a** | **2b** | **2c** | **2d** |

| Entry | Si source | Light source | 1a (%)[b] | 3a (%)[b] |
|---|---|---|---|---|
| 1 | **2a** | blue LEDs | 18 | 77 |
| 2 | **2b** | blue LEDs | 100 | nd |
| 3 | **2c** | blue LEDs | 100 | nd |
| 4 | **2d** | blue LEDs | 100 | nd |
| 5[c] | **2a** | blue LEDs | traces | 83 |
| 6[d] | **2a** | blue Kessil | nd | 99 (84)[e] |
| 7 | **2a** | dark | 100 | nd |
| 8[d] | – | blue Kessil | 100 | nd |

[a] Conditions: **1a** (0.10 mmol), **2** (0.12 mmol), MeCN (1.0 mL, c = 0.1 M), blue LEDs irradiation ($\lambda_{max}$ = 455 nm), 16 h. [b] Yields were determined by $^1H$ NMR analysis using 1,3,5-trimethoxybenzene as internal standard. [c] MeCN (0.5 mL, c = 0.2 M). [d] Blue Kessil ($\lambda_{max}$ = 440 nm). [e] Isolated yield. Abbreviations: nd, no detected.

a dipeptide (**3y**). Different biomolecules and pharmaceuticals provided the hydroamination products (**3z-ad**) in high yields, showing the potential of the method for late-stage functionalization. Isonitrile **1z** from leelamine, an inexpensive and commercially available diterpene amine extracted from pine bark,[23] was deaminated to abietatriene (**3z**), which has been used in the total synthesis of several compounds and is not commercially available.[24] Additionally, the hydrodeamination derivatives of deacetyllinezolid (**3aa**), 2-amino D-glucose (**3ab**),[25] rimantadine (**3ac**) and linagliptin (**3ad**) were obtained in high yields. The site selectivity observed for the linagliptin derivative is remarkable and no sign of addition of the silyl radical to the alkyne was observed.[26] Moreover, *N*-Boc piperidine **3a** was synthesized on gram scale in 96% yield, enhancing the synthetic utility of this protocol.

The efficiency and simplicity of the visible-light mediated hydrodeamination offers an ideal scenario to design a selective deuterodeamination protocol using (TMS)₃SiD (Scheme 2, bottom part). Deuterium (D) labelling is an important tool for drug discovery and development, because it allows the incorporation of a non-radioactive, stable isotopic tag into drug lead candidates. Additionally, deuterated pharmaceuticals often show better absorption, distribution, metabolism and elimination (ADME) properties.[27] When we substituted (TMS)₃SiH for (TMS)₃SiD the corresponding deuterodeamination products were obtained in good yields (**4a-f**). Interestingly, the deuterodeamination product derived from 2-amino D-glucose (**4c**)[25] places the deuterium atom exclusively in the axial position, which is in contrast with previous methods to prepare 2-deutero-2-deoxy-D-glucose **4c**.[28]
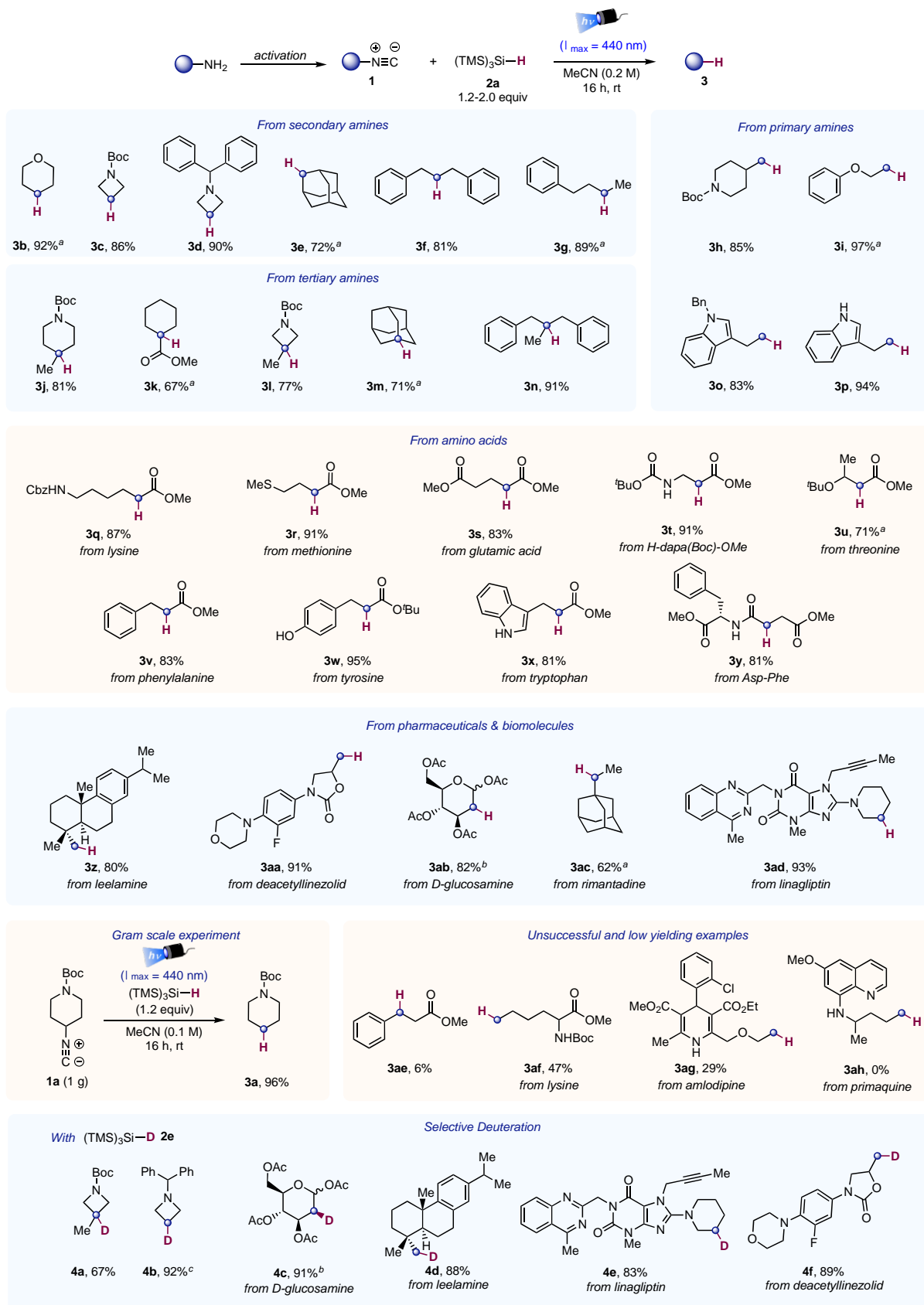
**Scheme 2.** Substrate Scope. Conditions: **1** (0.20 mmol), **2a** (0.24-0.40 mmol), MeCN (1.0 mL, c = 0.2 M), blue Kessil irradiation ($\lambda_{max}$ = 440 nm). [a] Yield was calculated by ^{1}H NMR using 1,3,5-trimethoxybenzene as internal standard. [b] α/β = 87/13. Deuterodeamination Conditions: **1** (0.20 mmol), **2e** (0.40 mmol), MeCN (1.0 mL, c = 0.2 M), blue Kessil irradiation ($\lambda_{max}$ = 440 nm). [c] 32 h.

While exploring the scope of the reaction, we noticed that benzylic substrates as well as some of the $C_\alpha$-1° isonitriles afforded the deamination products (**3ae-ah**) in low or neglectable yields. We decided to further optimize these results and found that the yields were dramatically improved when a catalytic amount (1-5 mol%) of 1,2,3,5-tetrakis(carbazol-9-yl)-4,6-dicyanobenzene (4CzIPN) was used as photosensitizer (Scheme 3). The examples of the $C_\alpha$-1° isonitriles **1af** and **1ah** derived from lysine and primaquine are especially noticeable providing the hydrodeamination products **3af** and **3ah** in 93% and 95% yield, respectively. We also run the photocatalyzed hydrodeamination in two isonitriles that worked well under the non-catalyzed conditions (**1a** and **1o**). With these compounds we observed a remarkable acceleration of the reaction revealing that a different mechanism was operating. To the best of our knowledge this is the first C-N cleavage from isonitriles using photocatalysis under visible-light irradiation.
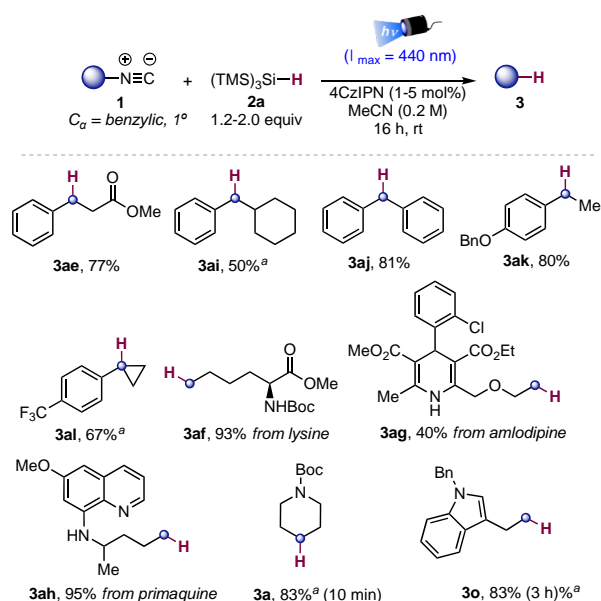


**Scheme 3.** Deamination in the presence of 4CzIPN. Conditions: **1** (0.20 mmol), **2a** (0.24-0.40 mmol), 4CzIPN (1-5 mol%), MeCN (1.0 mL, c = 0.2 M), blue Kessil irradiation ($\lambda_{max}$ = 440 nm). [a] Yield was calculated by $^1$H NMR using 1,3,5-trimethoxybenzene as internal standard.

To gain insight into the mechanism of the photoinduced hydrodeamination reaction, several mechanistic studies were performed. We focused first on the light-mediated hydrodeamination in the absence of a photocatalyst. To probe the intermediacy of radical species, we carried out the hydrodeamination in the presence of TEMPO (2,2,6,6-tetramethyl-1-piperidinyloxy) as a radical scavenger, observing a complete shutdown of the reaction (Figure 1A). When we changed isonitrile **1a** for *tert*-butyl acrylate the Giese product **5** was obtained in high yield. This result supports the formation of a silyl radical under visible-light irradiation. The analysis of the UV/Vis absorption spectra of each of the reaction components and mixtures in MeCN showed a small bathochromic shift. However, this new absorption band was allocated in the UV region and did not explain the photoactivation by blue light irradiation.[22] Additionally, a radical clock experiment was performed employing isonitrile **1am** which evolved to the corresponding open-chain product **3am**

in 78% yield under standard hydrodeamination conditions, which is in agreement with the formation of an alkyl radical intermediate from the isonitriles.

Given the mechanistic studies described herein and previous reports,[15,19] a plausible radical chain mechanism for this hydrodeamination protocol is proposed in Figure 1A. The initiation begins with the formation of the silyl radical **A** by light irradiation of tris(trimethylsilyl)silane (**2a**).[21] The addition of radical **A** to isocyanide **1** triggers the generation of an imidoyl radical intermediate **B**, which subsequently suffers a β–fragmentation to produce the alkyl radical **C**. At this point, the alkyl radical **C** reacts with another molecule of supersilane to afford the desired hydrodeamination product **3** through a hydrogen atom transfer (HAT) event. Finally, the silyl radical **A** generated after the HAT process propagates the radical chain mechanism. The deuterium (D) labeling studies shown in Scheme 2 support the hydrogen atom transfer (HAT) from silane **2a**. Additionally, the photochemical quantum yield (Φ) for this transformation in the absence of a photocatalyst is 132, which indicates a chain propagation mechanism.[29]

The above proposed radical chain mechanism is supported by Density Functional Theory (DFT) calculations carried out at the PCM(acetonitrile)-M06-2X/def2-TZVPP//PCM(acetonitrile)-M06-X/def2-SVP level (see supporting information for details). The computed reaction profiles shown in Figure 1C (using the model (H$_3$Si)$_3$Si system instead of (Me$_3$Si)$_3$Si)) indicate that the initial addition of the silyl radical to the isonitrile occurs with a low barrier of ca. 10.5 kcal/mol in a nearly thermoneutral reaction, regardless of the nature of the isonitrile (i.e. primary, secondary, tertiary or benzylic). This step leads to the formation of the corresponding imidoyl radical **INT1**, whose unpaired electron is, not surprisingly, mainly located at the carbon atom (see spin-density in Figure 1C). **INT1** then evolves into the respective alkyl radical **INT2** with concomitant release of a molecule of (H$_3$Si)$_3$Si-CN. This transformation proceeds through the transition state **TS2**, which is associated with the cleavage of the C-N bond (i.e. β-fragmentation). Interestingly, both the barriers (ΔG$^{\neq}$ in the range of 6.9 to 16.0 kcal/mol) and the reaction energies (ΔG$_R$ in the range of −8.7 to −21.2 kcal/mol) computed for this step nicely follow the expected trend of the relative stability of the alkyl radicals (i.e. primary < secondary < tertiary < benzylic). The high exergonicity of this β-fragmentation step compensates for the initial thermoneutral nature of the initial radical addition and drives the whole transformation forward. Finally, alkyl radicals **INT2** react with (H$_3$Si)$_3$Si-H via the transition states **TS3**, which are associated with the migration of a hydrogen atom from the supersilane to the alkyl radical (i.e. a HAT reaction), to afford, in an exergonic transformation, the corresponding hydrodeaminated products together with a new silyl radical which can promote a new radical chain process.

Then, we decided to get more insight into the role of the 4CzIPN in the photocatalyzed hydrodeamination. The reaction profile for compounds **1ae** and **1a** showed a clear acceleration of the reaction in the presence of the photocatalyst which is particularly striking for compound **1a** (83% yield after 10 min vs 4% after 15 min for **1a**, Figure 1B). Additionally, the Φ value for the photocatalyzed hydrodeamination of compound **1ae** is 1.1, which suggest that a different mechanism is operating.
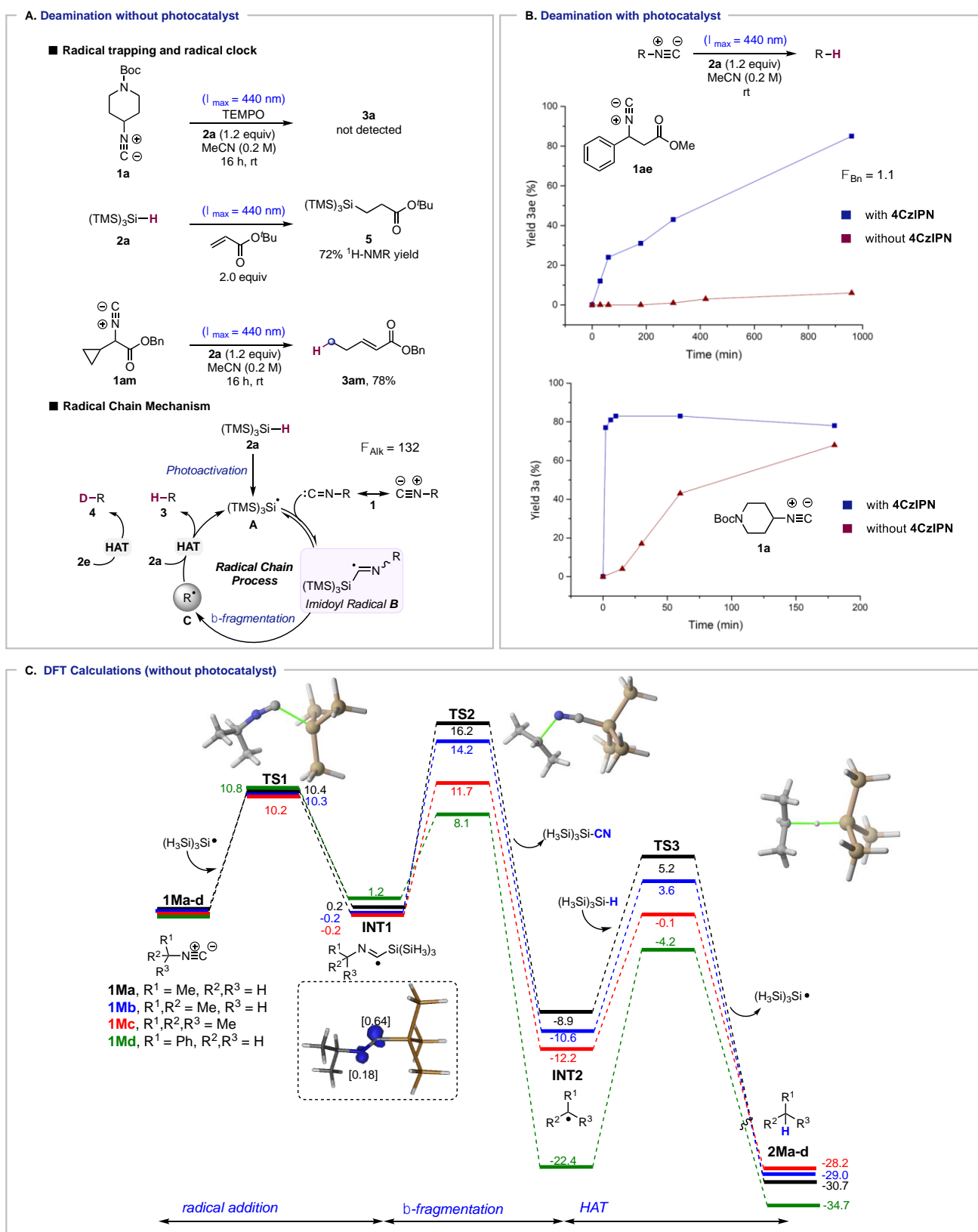
**Figure 1.** Mechanistic studies and DFT calculations.

For a better understanding on the excited state of the photosensitizer (PS) 4CzIPN and its kinetic implications on the overall reaction pathways, UV-vis absorption, steady-state and time-resolved photoluminescence (PL and TRPL, respectively), and transient absorption spectroscopy (TAS) experiments were performed.

First, we studied the photophysical properties of the 4CzIPN photocatalyst (see Supporting Information, section **Photophysical characterization of the photosensitizer 4CzIPN**). To determine the interaction between the excited states of 4CzIPN and the isonitrile substrates, PL, TRPL and TAS quenching experiments were performed employing model substrates **1a**, **1o** and the silane **2a** (Figure 2 and Supporting Information, section **Photophysical characterization of the photosensitizer 4CzIPN in the presence of 1a, 1o or 2a**). UV-vis absorption and fluorescence spectroscopies confirm the negligible overlapping between **1a**, **1o** or **2a** and the 4CzIPN bands after excitation at 440 nm, avoiding potential inner interferences from isonitrile or silane absorption/emission contribution (Figure S25).

Photoluminescence quenching experiments of 4CzIPN by addition of **1a** resulted in an efficient emission deactivation with quenching constant ($k_q$) of $3.6 \times 10^8$ M$^{-1}$ s$^{-1}$ (Figure 2A). In addition, no changes were observed in the maximum position of the emission spectra with the increase of the quencher concentration. Furthermore, new fluorescence bands are not observed, which rules out the formation of excimers and exciplexes.[30] Time-resolved analysis ($\lambda_{exc}$ = 445 nm, with a band-pass filter centered at 550 nm) confirmed the dynamic quenching (Figure 2B). The addition of the substrate **1a** quenched the two kinetic components (prompt and delayed decay) of 4CzIPN, obtaining similar quenching constants ($k_q$ = $2.23 \times 10^8$ and $1.47 \times 10^8$ M$^{-1}$ s$^{-1}$, respectively (Figure 2C). The model substrate **1o** exhibited quenching constant values of $k_q$ = $7.39 \times 10^9$ and $6.14 \times 10^9$ M$^{-1}$ s$^{-1}$ in PL and TRPL mode, respectively. A value of $k_q$ = $3.95 \times 10^9$ M$^{-1}$ s$^{-1}$ for the delayed decay contribution was obtained (Figure S26). These findings indicate that the fluorescence rate quenching of 4CzIPN by **1a** or **1o** is controlled by diffusion.[31]

The quenching of 4CzIPN employing silane **2a** was negligible and a solution mixture containing **1a** or **1o** with **2a** (silane and isonitrile at the same concentration) did not increase the quenching efficiency (Figure S27). This result is indicative of the preferably interaction between the photosensitizer and the isonitrile instead of the silane. Furthermore, the null difference in the $k_q$ value for the mixture of PS + **1a** (or **1o**) in the absence or presence of silane suggests a fast interaction between PS and isonitrile instead of formation of an imidoyl radical by addition of an *in-situ* formed silyl radical to the isonitrile, which is the proposed mechanism in the absence of the photocatalyst (Figure 1A).

Then, quenching studies were performed using TAS. First, no TAS signal was observed for **1a**, **1o** or **2a** in the ns-μs scale. Additionally, no TAS signal was observed in a solution mixture of **1a** or **1o** with **2a**. Therefore, the formation of an imidoyl radical cannot be confirmed using ns-TAS or perhaps is generated in the timescale outside our parameters. In addition, no changes in the TA of 4CzIPN were observed in a solution mixture of 4CzIPN + **2a**. However, the addition of **1a** or **1o** over 4CzIPN induces a continuous decrease of the 460 nm transient band for 4CzIPN, concomitantly with a growth between 520-650 nm with maximum at 580 nm (Figure 2D and S28). The new band was observed at low concentration of

isonitrile (from 2 mM in the case of **1o**), where no interference by isonitrile or silane absorption occurs after excitation at 440 nm. Thus, the transient band detected at 580 nm should be due to the interaction of the PS with **1a** or **1o**, showing residual 4CzIPN* 460 nm peak (Figure 2D, inset). The resulted transient is identical independently of the isonitrile used. This new transient was observed both in aerated as well as deaerated solutions (Figure S29).

To investigate the nature of the new transient band centered at 580 nm, different scenarios were evaluated: formation of a charge-transfer donor-acceptor complex, energy transfer (ET) or electron transfer (eT) processes.[32] The formation of a charge-transfer (CT) donor-acceptor complex could generate a new TA via two pathways: i) an exciplex formation between isonitriles **1a** or **1o** with the excited 4CzIPN or, ii) the formation of an electron-donor-acceptor (EDA) complex between the isonitrile and 4CzIPN.[18] These two processes were discarded since we did not observe the formation of a new fluorescence emission (Figures 2A and S26A) and/or red-shifted absorption band (Figures S7-S10).[33]

Regarding energy transfer catalysis, Förster Resonance Energy Transfer (FRET, from the singlet excited state) and Dexter process (from the singlet or triplet excited state) are the two main mechanisms that could be involved.[34,35] A FRET mechanism is discarded since no spectral overlap between the fluorescence of 4CzIPN and the absorption of either **1a**, **1o** or **2a** is observed.[36,37] Since the substrates employed absorb only at short wavelengths, it is expected that a Dexter ET would be not favorable. Moreover, the calculated triplet state energy for an isonitrile (~110 kcal mol$^{-1}$) is higher than that for 4CzIPN (58.4 kcal mol$^{-1}$)[38] Although a non-vertical ET process cannot be ruled out,[39,40] we do not have any experimental evidence to support this idea. Moreover, the rapid reverse ISC (T$_1$ to S$_1$) and the resultant thermally activated delayed fluorescence (TADF) inevitably presents significant competition to a hypothetical intermolecular triplet–triplet energy transfer (TTET) between the photosensitizer and **1a** or **1o**, particularly under the diffusion limited conditions. Consequently, TTET does not seem a likely scenario in this transformation.[41]

We then considered the possibility of an electron transfer process between the isonitrile and the excited state of 4CzIPN to produce the corresponding anionic and cationic radicals. To evaluate the generation of radical species by electron transfer, transient lifetimes analysis for 4CzIPN in absence and presence of the isonitrile were performed (Figure 2F). The new photogenerated species showed a three-exponential fit with a first contribution of 5.7 μs; a second shorter lifetime of 223 ns and a longer lifetime above 50 μs (Figure S31A). In addition, the 460 nm signal was strongly quenched, accompanied of the appearance of a large second τ (Figure S31B). It has been reported that 4CzIPN is able to induce both oxidative and reductive reactions.[42–44] Therefore, the new signal could correspond to the photochemical generation of the radical cation or anion of 4CzIPN. To get further insight, 1,4-diazabicyclo[2.2.2]octane (DABCO) and antimony pentachloride (SbCl$_5$) were employed in the presence of 4CzIPN as electron donor and acceptor respectively, to investigate if an oxidative or reductive quenching cycle is involved. DABCO is a good electron donor (0.8 V *vs*. NHE)[45] and a common reductive quencher to generate the corresponding radical anion of a molecule.[46] As observed in Figure 2G, the resulted TA spectrum is different to those

obtained in Figure 2D. Therefore, the reaction does not seem to be driven by a reductive quenching cycle. Similar experiments were performed with $SbCl_5$ as oxidative quencher of 4CzIPN (Figure 2H). Interestingly, we observed a transient absorption analogous to those recorded in Figure 2D. These data are also in agreement to those reported for a related carbazole radical cation (TA maximum at ca. 550-600 nm). [47]
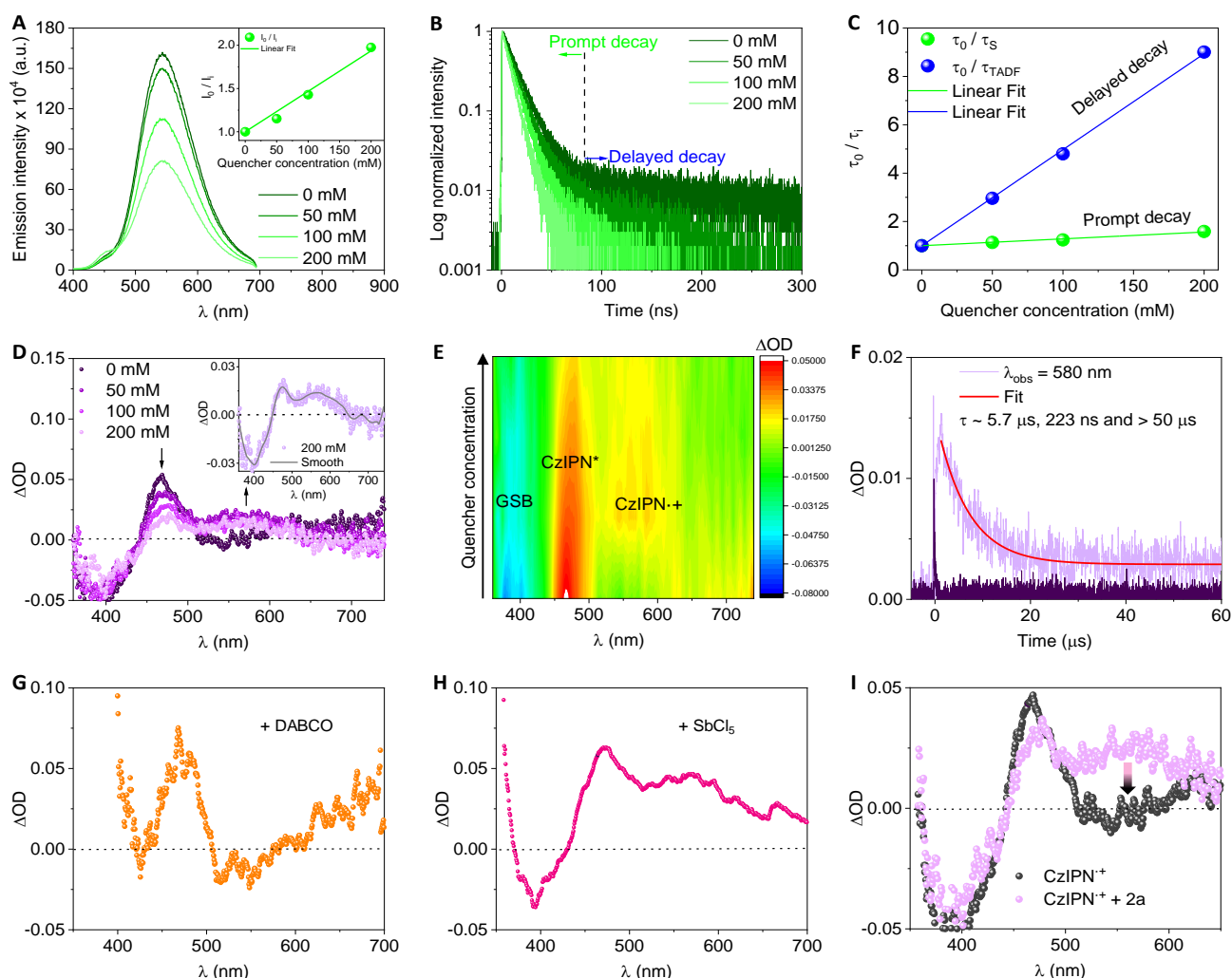


**Figure 2.** Steady-state photoluminescence, time-resolved photoluminescence and transient absorption spectroscopy quenching studies for 4CzIPN in acetonitrile. A) Photoluminescence spectra ($\lambda_{exc}$ = 440 nm) for 4CzIPN with increasing addition concentration of substrate **1a** (up to 200 mM). Inset: Stern-Volmer plot. B) Corresponding time-resolved photoluminescence traces ($\lambda_{exc}$ = 445 nm, band-pass filter at 550 nm) for 4CzIPN under the same conditions. C) Stern-Volmer plots for the photoluminescence experiments. D) Transient absorption spectra (TAS, $\lambda_{exc}$ = 440 nm, $N_2$) after photoluminescence subtraction for CzIPN with increasing addition concentration of substrate **1a** (up to 200 mM). Inset: Zoom image. E) TAS colour mapping ($\lambda_{exc}$ = 440 nm, $N_2$) under the same conditions. F) Transient lifetime traces ($\lambda_{exc}$ = 440 nm, $\lambda_{obs}$ = 580 nm, $N_2$) for CzIPN in the absence (black) or presence (purple) of 200 mM of the substrate **1a**. The fit is included (red). G and H) Transient absorption spectrum after excitation with 440 nm laser pulses of a solution containing G) 4CzIPN + DABCO or H) 4CzIPN + $SbCl_5$ in $N_2$-saturated acetonitrile. The data were recorded after 2 $\mu$s laser pulse. I) Transient absorption spectra (TAS, $\lambda_{exc}$ = 440 nm, $N_2$) with luminescence subtraction for 4CzIPN·+ with addition concentration of **2a** (200 mM). 4CzIPN·+ was previously prepared by addition of **1o** (10 mM) or $SbCl_5$. The data were recorded after 2 $\mu$s laser pulse.

The solid photophysical experimental evidence strongly supports the participation of the excited state of the photocatalyst in the photoinduced reaction between 4CzIPN and the substrates **1a** or **1o**. Detection of a transient radical which could correspond to the generation of 4CzIPN·+, the oxidized species derived from the photocatalyst, is clearly in favor of an oxidative quenching cycle via a photo-induced electron transfer mechanism. Since the observed TAS for 4CzIPN cover all spectral window, the associated band to the radical anion of **1a** or **1o** could not be detected. The single electron reduction of isonitriles has been previously proposed using sodium naphthalene as reductant.[48] However, there is

no data available in the literature on the redox potential of these compounds. We tried to measure the reduction potential of *tert*-butyl isonitrile using cyclic voltammetry. Unfortunately, despite our efforts, we did not observe any reduction peak that could support the experimental evidence, which suggest that there might be other factors involved in the electron transfer.

Finally, to evaluate the role of supersilane **2a** in an oxidative quenching cycle, quenching experiments of the new transient band centered at 580 nm were performed. To do this, once the radical species was generated by means of addition of isonitrile or with the oxidant $SbCl_5$, a large amount of **2a** was added (up to 200 mM). Interestingly, the band at 580 nm was

quenched, resulting in a TA spectrum identical to the pristine photocatalyst (Figure 2l).

Although not conclusive, all these findings point towards a mechanism in which upon excitation of the 4CzIPN with visible light, the excited state of 4CzIPN is efficiently populated and able to sensitize the isonitrile substrate through what appears to be a single electron transfer. The radical anion generated upon reduction of the isonitrile could undergo β-fragmentation to generate a carbon centered radical and a cyanide anion, similar to that proposed using sodium naphthalene.[48] Once the carbon centered radical is formed it could then react with the silane through hydrogen atom transfer to provide the deamination product. The silyl radical generated after HAT could be oxidized by 4CzIPN•+ to a silyl cation[49] eventually trapped by the cyanide anion, regenerating the ground-state catalyst. Further mechanistic studies will be needed to fully support this hypothesis and are the subject of ongoing studies.

In summary, we have developed an efficient and operationally simple photoinduced hydrodeamination protocol of primary, secondary, and tertiary isonitriles. The reaction shows a broad functional group compatibility and potential to be used in late-stage functionalization. The use of a deuterated silane allows for the site-selective deuteration of the C-N bond. Although most examples only require visible-light irradiation of the isonitrile in the presence of a silyl radical precursor, we observed a dramatic acceleration of the reaction in the presence of an organic photocatalyst which was indicative of a change in the mechanism involved. Mechanistic studies using UV-vis absorption, steady-state and time-resolved photoluminescence, and transient absorption spectroscopy suggest that the excited state of 4CzIPN is able to sensitize the isonitrile through a single electron transfer.

Beyond the dehydrodeamination reaction, our study shows the feasibility to generate an alkyl radical from an isonitrile under visible-light irradiation. We believe this finding will open the door to design novel deamination protocols using isonitriles as primary alkyl amine derivatives.

## Acknowledgements

## Conflict of Interest

The authors declare no conflict of interest.

## Supporting Information

Materials and methods, experimental procedures, complete computational details, $^1$H and $^{13}$C NMR spectra, and HRMS data are available in the Supporting Information.

## References

[1]  a) J. D. Bell, J. A. Murphy, *Chem. Soc. Rev.* **2021**, *50*, 9540-9685. b) R. Cannalire, S. Pelliccia, L. Sancineto, E. Novellino, G. C. Tron, M. Giustiniano, *Chem. Soc. Rev.* **2021**, *50*, 766-897. c) L. Marzo, S. K. Pagire, O. Reiser, B. König, *Angew. Chem. Int. Ed.* **2018**, *57*, 10034-10072. d) C. Stephenson, T. Yoon, D. W. C. MacMillan, *Visible Light Photocatalysis in Organic Chemistry*, Wiley-VCH Verlag GmbH & Co. KGaA, Weinheim, Germany, **2018**, p 456.

[2]  Y. Wang, I. Haight, R. Gupta, A. Vasudevan, *J. Med. Chem.* **2021**, *64*, 17115-17122.

[3]  a) Y. Gao, S. Jiang, N. D. Mao, H. Xiang, J. L. Duan, X. Y. Ye, L. W. Wang, Y. Ye, T. Xie, *Top Curr Chem* **2022**, *380:25*, doi: 10.1007/s41061-022-00381-x. b) K. J. Berger, M. D. Levin, *Org. Biomol. Chem.* **2021**, *19*, 11-36. c) Y.-N. Li, F. Xiao, Y. Guo, Y.-F. Zeng, *Eur. J. Org. Chem.* **2021**, *2021*, 1215-1228. d) F.-S. He, S. Ye, J. Wu, *ACS Catal.* **2019**, *9*, 8943-8960. e) D. Kong, P. J. Moon, R. J.; Lundgren, *Nat. Catal.* **2019**, *2*, 473-476.

[4]  C. H Basch, J. Liao, J. Xu, J. J. Piane, M. P. Watson, *J. Am. Chem. Soc.* **2017**, *139*, 5313-5316.

[5]  Selected transition-metal catalyzed transformations using pyridinium salts: a) X. Zhang, D. Qi, C. Jiao, X. Liu, G. Zhang, *Nat. Commun.* **2021**, *12*, 4904-4912. b) M. E. Hoerrner, K. M. Baker, C. H. Basch, E. M. Bampo, M. P. Watson, *Org. Lett.* **2019**, *21*, 7356-7360. c) R. Martin-Montero, V. R. Yatham, H. Yin, J. Davies, R. Martin, *Org. Lett.* **2019**, *21*, 2947-2951. d) S. Ni, C. X. Li, Y. Mao, J. Han, Y. Wang, H. Yan, Y. Pan, *Sci. Adv.* **2019**, *5*, eaaw9516. e) H. Yue, C. Zhu, L. Shen, Q. Geng, K. J. Hock, T. Yuan, L. Cavallo, M. Rueping, *Chem. Sci.* **2019**, *10*, 4430-4435. f) J. Hu, B. Cheng, X. Yang, T. P. Loh, *Adv. Synth. Catal.* **2019**, *361*, 4902-4908. g) K. M. Baker, D. Lucas Baca, S. Plunkett, M. E. Daneker, M. P. Watson, *Org. Lett.* **2019**, *21*, 9738-9741. h) S. Plunkett, C. H. Basch, S. O. Santana, M. P. Watson, *J. Am. Chem. Soc.* **2019**, *141*, 2257-2262. i) S. Z. Sun, C. Romano, R. Martin, *J. Am. Chem. Soc.* **2019**, *141*, 16197-16201. j) W. Guan, J. Liao, M. P. Watson, *Synthesis* **2018**, 50, 3231-3237. k) J. Hu, G. Wang, S. Li, Z. Shi, *Angew. Chem., Int. Ed.* **2018**, *57*, 15227-15231.

[6]  F. J. R. Klauck, M. J. James, F. Glorius, *Angew. Chem., Int. Ed.* **2017**, *56*, 12336-12339.

[7]  Selected photocatalyzed transformations using pyridinium salts: a) T. Yang, Y. Wei, M. J. Koh, *ACS Catal.* **2021**, *11*, 6519-6525. b) C. Wang, R. Qi, H. Xue, Y. Shen, M. Chang, Y. Chen, R. Wang, Z. Xu, *Angew. Chem., Int. Ed.* **2020**, *59*, 7461-7466. c) Q. Xia, Y. Li, X. Wang, P. Dai, H. Deng, W.-H. Zhang, *Org. Lett.* **2020**, *22*, 7290-7294. d) M. J. James, F. Strieth-Kalthoff, F. Sandfort, F. J. R. Klauck, F. Wagener, F. Glorius, *Chem. Eur. J.* **2019**, *25*, 8240-8244. e) J. Yi, S. O. Badir, L. M. Kammer, M. Ribagorda, G. A. Molander, *Org. Lett.* **2019**, *21*, 3346-3351. f) X. Jiang, M. M. Zhang, W. Xiong, L. Q. Lu, W. J. Xiao, *Angew. Chem., Int. Ed.* **2019**, *58*, 2402-2406. g) Z. K. Yang, N. X. Xu, C. Wang, M. Uchiyama, *Chem. Eur. J.* **2019**, *25*, 5433-5439. h) J. Wu, P. S. Grant, X. Li, A. Noble, V. K. Aggarwal, *Angew. Chem. Int. Ed.* **2019**, *131*, 5753-5757. i) F. J. R. Klauck, H. Yoon, M. J. James, M. Lautens, F. Glorius, *ACS Catal.* **2019**, *9*, 236-241. j) J. Wu, L. He, A. Noble, V. K. Aggarwal, *J. Am. Chem. Soc.* **2018**, *140*, 10700-10704. k) F. Sandfort, F. Strieth-Kalthoff, F. J. R. Klauck, M. J. James, F. Glorius, *Chem. Eur. J.* **2018**, *24*, 17210-17214.

[8]  a) J. Annibaletto, C. Jacob, C. Theunissen, *Org. Lett.* **2022**, *24*, 4170-4175. b) M. Miao, L.-L. Liao, G.-M. Cao, W.-J. Zhou, D.-G. Yu, *Sci. China Chem.* **2019**, *62*, 1519-1524. c) L. L. Liao, G. M. Cao, J. H. Ye, G. Q. Sun, W. J. Zhou, Y. Y. Gui, S. S. Yan, G. Shen, D. G. Yu, *J. Am. Chem. Soc.* **2018**, *140*, 17338-17342.

[9]  M. A. Ashley, T. Rovis, *J. Am. Chem. Soc.* **2020**, *142*, 18310-18316.

[10] J. R. Dorsheimer, M. A. Ashley, T. Rovis, *J. Am. Chem. Soc.* **2021**, *143*, 19294-19299.

[11] a) K. A. Steiniger, M. C. Lamb, T. H. Lambert, *J. Am. Chem. Soc.* **2023**, *145*, 11524-11529. b) D. Chattapadhyay, A. Aydogan, K. Doktor, A. Maity, J. W. Wu, Q. Michaude, *ACS Catal.* **2023**, *13*, 7263-7268.

[12] a) M. J. Schnermann, R. A. Shenvi, *Nat. Prod. Rep.*, **2015**, *32*, 543–577. b) A. Massarotti, F. Brunelli, S. Aprile, M. Giustiniano, G. C.

Tron, *Chem. Rev.* **2021**, *121*, 10742−10788. c) R. M. Hohlman, D. H. Sherman*, Nat. Prod. Rep.*, **2021**, *38*, 1567–1588.

[13] a) Y.-X. Si, P.-F. Zhu, S.-L. Zhang, *Org. Lett.* **2020**, *22*, 9086-9090. b) K. A. Waibel, R. Nickisch, N. Möhl, R. Seimb, M. A. R. Meier, *Green Chem.*, **2020**, *22*, 933–941.|

[14] V. G. Nenajdenko, *Isocyanide Chemistry: Applications in Synthesis and Material Science*; Wiley-VCH.; Weinheim, Germany, **2012**.

[15] a) D. H. R. Barton, G. Bringmann, G. Lamotte, W. B. Motherwell, R. S. H. Motherwell, A. E. A. Porter, *J. Chem. Soc., Perkin Trans. 1,* **1980**, 2657-2664. b) D. H. R. Barton, G. Bringmann, G. Lamotte, R. S. H. Motherwell, W. B. Motherwell, *Tetrahedron Lett.* **1979**, *24*, 2291-2294. c) T. Saegusa, S. Kobayashi, Y. Ito, N. Yasuda, *J. Am. Chem. Soc.* **1968**, *90*, 4182.

[16] Four examples using supersilane instead of Bu₃SnH have been described using simple alkyl isonitriles. These reactions still required heating in refluxing benzene or toluene, a radical initiator and an excess of silane. The functional group compatibility has not been demonstrated. M. Ballestri, C. Chatgilialoglu, *J. Org. Chem.* **1991**, *56*, 678-683.

[17] Selected examples of silyl radical generation and use in visible-light mediated transformations: a) S. Mistry, R. Kumar, A. Lister, M. J. Gaunt, *Chem. Sci.*, **2022**, *13*, 13241–13247. b) J. H. Blackwell, R. Kumar, M. J. Gaunt, *J. Am. Chem. Soc.* **2021**, *143*, 1598-1609. c) R. Roopender Kumar, N. J. Flodén, W. G. Whitehurst, M. J. Gaunt, *Nature* **2020**, *581*, 415−420. d) D. J. P. Kornfilt, D. W. C. MacMillan, *J. Am. Chem. Soc.* **2019**, *141*, 6853-6858. e) C. Le, T. Q. Chen, T. Liang, P. Zhang, D. W. C. MacMillan, *Science* **2018**, *360*, 1010-1014. f) P. Zhang, C. Le, D. W. C. MacMillan, *J. Am. Chem. Soc.* **2016**, *138*, 8084-8087. g) H. Jiang, J. R. Bak, F. J. López-Delgado, K. A. Jørgensen, *Green Chem.* **2013**, *15*, 3355-3359.

[18] C. Russo, J. Amato, G. C. Tron, M. Giustiniano, *J. Org. Chem.* **2021**, *86*, 18117-18127.

[19] M. Minozzi, D. Nanni, P. Spagnolo, *Current Organic Chemistry* **2007**, *11*, 1366-1384.

[20] a) H. Fang, M. Oestreich, *Angew. Chem., Int. Ed.* **2020**, *59*, 11394-11398. This protocol is only suitable for benzylic and α-tertiary amines. b) K. J. Berger, J. L. Driscoll, M. Yuan, B. D. Dherange, O. Gutierrez, M. D. Levin, *J. Am. Chem. Soc.* **2021**, *143*, 17366−17373. This protocol is not suitable for benzylic and α-tertiary amines.

[21] The generation of silyl radicals under visible light irradiation in the absence of a photocatalyst has been observed before but there is no conclusive evidence that unravels the initiation pathway. See for example, ref. 17a, 17b and 17g.

[22] See Supporting Information for more details.

[23] W. J. Gottstein, L. C. Cheney, *J. Org. Chem.* **1965**, *30*, 2072-2073.

[24] N. Mori, K. Kuzuya, H. Watanabe, *J. Org. Chem.* **2016**, *81*, 11866-11870.

[25] We did not observed erosion of the stereochemistry in the anomeric carbon. Compounds **3ab** and **4c** were obtained as an 87/13, α/β mixture of anomers starting from the same anomeric mixture in the corresponding isonitrile.

[26] a) S. Ghosh, D. Lai, A. Hajra, *Org. Biomol. Chem.* **2021**, *19*, 2399-2415. b) J.-S. Li, J. Wu, *ChemPhotoChem* **2018**, *2*, 839-846.

[27] a) J. Atzrodt, V. Derdau, T. Fey, J. Zimmermann, *Angew. Chem., Int. Ed.* **2007**, *46*, 7744-7765. b) J. Atzrodt, V. Derdau, W. J. Kerr, M. Reid, *Angew. Chem., Int. Ed.* **2018**, *57*, 1758-1784. c) T. Pirali, M. Serafini, S. Cargnin, A. A. Genazzani, *J. Med. Chem.* **2019**, *62*, 5276-5297.

[28] I. Fokt, S. Skora, C. Conrad, T. Madden, M. Mark Emmett, W. Priebe, *Carbohydr. Res.* **2013**, *368*, 111-119.

[29] M. A. Cismesia, T. P. Yoon, *Chem. Sci.* **2015**, *6*, 5426-5434.

[30] B. T. Lim, S. Okajima, E. C. Lim, *J. Chem. Phys.* **1986**, *84*, 1937-1939.

[31] E. Nuin, M. Gomez-Mendoza, M. L. Marin, I. Andreu, M. A. Miranda, *J. Phys. Chem. B* **2013**, *117*, 9327-9332.

[32] A HAT process was also discarded running the TA spectrum of 4CZIPN in the presence of isopropanol as HAT donor (see Figure S33). The transient band at 580 nm was not observed under those conditions.

[33] Z.-Y. Cao, T. Ghosh, P. Melchiorre, *Nat. Commun.* **2018**, *9*, 3274.

[34] J. Corpas, M. Gomez-Mendoza, J. Ramírez-Cárdenas, V. A. de la Peña O'Shea, P. Mauleón, R. Gómez Arrayás, J. C. Carretero, *J. Am. Chem. Soc.* **2022**, *144*, 13006-13017.

[35] T. Neveselý, M. Wienhold, J. J. Molloy, R. Gilmour, *Chem. Rev.* **2022**, *122*, 2650-2694.

[36] F. Strieth-Kalthoff, M. J. James, M. Teders, L. Pitzer, F. Glorius, *Chem. Soc. Rev.* **2018**, *47*, 7190-7202.

[37] A. A. Abdel-Shafi, D. R. Worrall, J. *Photochem. Photobiol. A Chem.* **2005**, *172*, 170-179.

[38] J. Lu, B. Pattengale, Q. Liu, S. Yang, W. Shi, S. Li, J. Huang, J. Zhang, *J. Am. Chem. Soc.* **2018**, *140*, 13719-13725.

[39] T. J. B. Zähringer, M. Wienhold, R. Gilmour, C. Kerzig, *J. Am. Chem. Soc.* **2023**, *145*, 21576-21586.

[40] J. Corpas, M. Gomez-Mendoza, E. M. Arpa, V. A. de la Peña O'Shea, B. Durbeej, J. C. Carretero, P. Mauleón, R. G. Arrayás, *ACS Catal.* **2023**, 14914-14927.

[41] J. Peng, X. Guo, X. Jiang, D. Zhao, Y. Ma, *Chem. Sci.* **2016**, *7*, 1233-1237.

[42] E. Speckmeier, T. G. Fischer, K. Zeitler, *J. Am. Chem. Soc.* **2018**, *140*, 15353-15365.

[43] F. Mohamadpour, *RSC Adv.* **2023**, *13*, 2514-2522.

[44] T.-Y. Shang, L.-H. Lu, Z. Cao, Y. Liu, W.-M. He, B. Yu, *Chem. Commun.* **2019**, *55*, 5408-5419.

[45] M. J. Oddy, D. A. Kusza, W. F. Petersen, *Org. Lett.* **2021**, *23*, 8963-8967.

[46] J. Grover, G. Prakash, C. Teja, G. K. Lahiri, D. Maiti, *Green Chem.* **2023**, *25*, 3431-3436.

[47] W. Xie, J. Xu, U. Md Idros, J. Katsuhira, M. Fuki, M. Hayashi, M. Yamanaka, Y. Kobori, R. Matsubara, *Nat. Chem.* **2023**, *15*, 794-802.

[48] G. E. Niznik, H. M. Walborsky, *J. Org. Chem.* **1978**, *43*, 2396-2399.

[49] X.-J. Tang, Z. Zhang, W. R. Dolbier, *Chem. Eur. J.* **2015**, *21*, 18961-18965.